The use of MSC derived hepatocyte-like cells in microfluidic culture systems: an approach for studying the metabolic syndrome

Rodrigues, J.S.[1, 2], Cipriano, M. [2], Miranda, J. P. [2]

Abstract The metabolic syndrome, or insulin resistance syndrome, affects approximately one quarter of the world population. Three cell types are involved in its pathophysiology: adipocytes, myofibroblasts and hepatocytes. Therefore, understanding the role of cell-to-cell interactions in the development of this disease is crucial. The use of microfluidic devices has several advantages including the possibility to study the communication between different cell types. Thus, this work focused on the adaption of hepatocyte-like cells (HLCs) derived from human umbilical cord matrix mesenchymal stem cells, to a microfluidic device, and to evaluate HLCs energy metabolism. Herein, we were able to adapt the hepatic differentiation procedure to the microfluidic device and to maintain functional HLCs up to two weeks. Phase I and II biotransformation activities, glycogen storage, presence of hepatic markers (CK-18, ALB, HNF-4α, OATP-C and MRP2) and urea and albumin production were observed throughout this period. Most importantly, HLCs expressed genes regarding glycolysis and lipogenesis (*PDK4*), gluconeogenesis (*PEPCK* and *G6PASE*), fatty acid oxidation (*PPARA*), bile acid metabolism (*FXR* and *CYP7A1*) and mitochondrial function and biogenesis (*PGC-1A*) with similar trend to that observed in a physiologic context, in response to insulin and glucagon, and adapt their metabolism to fasting. To conclude, it was possible to obtain functional HLCs, maintaining its characteristics throughout culture time in parallel with the response to hormonal stimuli, setting up the roads for the possibility of using these cells to study cell-to-cell interactions in this microfluidic device.

Keywords: Glucagon; Hepatocyte-like cells; Insulin; Metabolic Syndrome; Microfluidic Devices

I. Introduction

The International Diabetes Federation estimates that a quarter of the adults worldwide suffers from metabolic syndrome. It is associated with the development of cardiovascular diseases and the risk of developing type II diabetes is increased by 5-fold compared with healthy people [1]. The metabolic syndrome is a combination of obesity, dyslipidaemia, insulin resistance and hypertension [2]. The main mechanism of its pathophysiology is insulin resistance (metabolic syndrome is also known as insulin resistance syndrome) due to an increase of circulating free fatty acids, released from an expanded mass of adipose tissue. Liver, skeletal muscle and adipose tissue cells become progressively less sensitive to insulin. Ultimately, glucose absorption no longer occurs [1].

Glucose is both a substrate and an end product for cells. Therefore, two opposite states need to be considered: high glucose (fed state) and low glucose (fasting or starvation) [3] (Figure 1). In the fed state, glucose, fatty acids and amino acids absorbed into the bloodstream reach the liver through the portal vein. Glucose is converted into pyruvate, through glycolysis, in the cytoplasm, being oxidized, through the tricarboxylic acid (TCA) cycle and oxidative phosphorylation in the mitochondria, to produce adenosine triphosphate (ATP). If energy is not needed, glucose is stored as glycogen or converted into fatty acids and amino acids in the liver. Hepatocytes generate triacylglycerol (TAG) through free fatty acid esterification. TAG is then stored in lipid droplets or secreted as very low density lipoproteins (VLDL), into circulation. Amino acids are used to synthesize proteins, glucose or other biomolecules [4]. These functions are controlled by insulin. It stimulates the uptake of glucose by peripheral tissues, glycolysis, energy storage and anabolic reactions, namely glycogen synthesis (glycogenesis) in liver and muscle, and fatty acid synthesis in liver and adipose tissue, in the fed state [3]. Insulin also suppresses an isoform of pyruvate dehydrogenase kinase (PDK4), thus increasing pyruvate consumption and glycolysis [5]. In fact, fasted PDK4 knockout mice present hypoglycaemia, since pyruvate enters TCA cycle for complete oxidation, thus not being available as a gluconeogenic substrate [6]. In the liver, insulin blocks glycogenolysis and gluconeogenesis [7]. On the other hand, in the fasted state, glucagon is released provoking a rise in intracellular cyclic adenosine monophosphate (cAMP), in the liver. The alteration of cAMP levels is the main mechanism by which liver releases glucose in the blood, through the induction of gluconeogenesis and glycogenolysis [8]. The increase in cAMP levels in liver [9] induces the expression of glucose 6-phosphatase (*G6Pase*), cytoplasmic phosphoenolpyruvate carboxylase (*PEPCK*) and peroxisome proliferator γ-activated receptor coactivator 1-α (*PGC-1A*) [4]. PGC-1α was shown to be elevated in the fasted state and in disease models of diabetes and insulin resistance [10], stimulating gluconeogenesis. β oxidation of fatty acids is then induced. Peroxisome proliferator-activated receptor α (PPARα), the main regulator of β oxidation, promotes it both in the mitochondria and peroxisomes through interaction with PPARα [11]. This has been demonstrated in *in vivo* studies where deletion of PPARα in mice showed a massive lipid accumulation in the liver, hypoglycaemia and elevated plasma free fatty acid levels [12]. Protein degradation occurs during prolonged starvation, which can serve as gluconeogenic substrates [4]. Bile acids regulate cholesterol homeostasis and contribute to the digestion and lipid absorption. The synthesis of bile acids, which takes place in the liver, contributes to the conversion of the hydrophobic cholesterol to a more water-soluble molecule. The first and rate-limiting step in the classic pathway of bile synthesis is catalysed by the cytochrome P450 enzyme cholesterol 7α-hydroxylase (CYP7A) [13]. Farnesoid X receptor (FXR) senses bile acids and responds by inhibiting its

[1] Instituto Superior Técnico, Universidade de Lisboa, Av. Rovisco Pais, Nº 1, 1049-001 Lisboa, Portugal
[2] Research Institute for Medicines (iMed.ULisboa), Faculty of Pharmacy, Universidade de Lisboa, Av. Prof. Gama Pinto, 1649-003 Lisbon, Portugal

synthesis [3], since its accumulation beyond a certain level becomes cytotoxic [13]. Therefore, FXR downregulates a CYP7A isoform, CYP7A1 [13]. 90 % of bile acids are reabsorbed in the intestine and return to the liver. Thus, in the fed state, high amounts of bile acids reach the liver through the portal vein. Upon starvation, there is a decrease in the levels of circulating bile acids [14]. In rat hepatocytes, insulin was shown to negatively regulate FXR gene expression [15]. On CYP7A1, insulin was shown to have a dual effect: physiological insulin concentrations rapidly induce *CYP7A1* expression while prolonged insulin treatment represses it [16]. However, there is no consensus regarding bile acids regulation by PGC-1α. There are reports that *FXR* is induced by PGC-1α [17,18] and the latter is elevated in fasting conditions. Therefore, CYP7A1 expression is decreased due to inhibition by FXR. On the other hand, some authors claim that PGC-1α interacts with *CYP7A1* promoter [14]. Thus, after prolonged fasting, *CYP7A1* transcription increases, helping to prepare the gastrointestinal tract for a future meal [14].

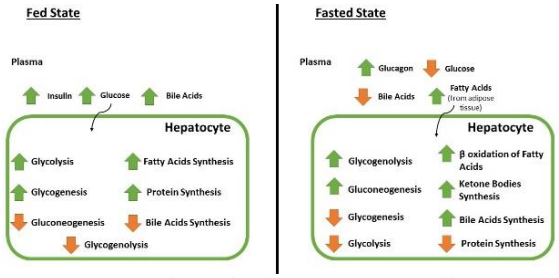

Figure 1 - Overview of the fed/fasted states: the effect in hepatocyte metabolism.

Two-dimensional (2D) traditional models do not mimic *in vivo* cellular organization, but most importantly do not involve interaction with other cell types and do not present media flows as what happens *in vivo* [19,20]. Microfluidic devices, on the other hand, are now being used due to its low reactant consumption, the possibility of modelling important aspects of microenvironment, such as creating medium flows and, according to its design, it may allow culturing of different types of cells in parallel. These devices are a possibility to overcome the limitations of current methods, introducing the organ-on-a-chip concept [21]. Therefore, microfluidic devices would be an interesting approach to study cell-to-cell interactions that can be regulated by secreting cellular factors or direct contact. Besides, cell–cell interaction within same or different cell types is another essential part of microenvironment making these devices important candidates for studying the metabolic syndrome where the interaction between liver cells, adipocytes and myofibroblasts is essential. Human primary hepatocytes cannot be maintained in culture during a reasonable time in order to allow long-term studies of cellular interaction [19]. Alternatively, hepatocyte-like cells (HLCs) derived from human stem cells are a fundamental source for biomedical applications [19]. In fact, our group has previously developed a hepatic differentiation protocol of human neonatal mesenchymal stem cells (hnMSCs) for obtaining competent HLCs that were able to be maintained in culture for more than 2 weeks [20,22]. Herein, we tested if such HLCs were able to adapt to a microfluidic device. Moreover, we evaluated if they were able to regulate their energy metabolism in response to fasting and to respond to insulin and glucagon stimuli, presenting the same trend observed physiologically. Thus, we studied the expression of key genes involved in glycolysis and lipogenesis regulation, gluconeogenesis, lipolysis, fatty acids metabolism, bile acids metabolism and mitochondrial function and biogenesis.

MATERIALS AND METHODS

Reagents

Cell culture supplements were purchased from Lonza, unless otherwise stated. Trypsin-EDTA, fetal bovine serum (FBS), insulin-transferrin-selenium solution (ITS), non-essential amino acids supplement (NEAA), rat-tail type I collagen and human insulin were purchased from Gibco®/Life Technologies. 7- ethoxyresorufin and 7-ethoxycoumarin were purchase from Alfa Aesar. Hepatocyte growth factor (HGF), fibroblast growth factors (FGF-2 and FGF-4) and oncostatin-M (OSM) were purchased from Peprotech. Finally, Iscove's modified Dulbecco's medium (IMDM), alpha modified Eagle's medium (α-MEM), epidermal growth factor (EGF), dexamethasone, DMSO, nicotinamide, 5-AZA, trypan blue, periodic acid, Schiff's reagent, Mayer's hematoxylin, amylase, Hank's balanced salt solution (HBSS), 4-methylumbelliferone (4-MU), β-glucuronidase/arylsulfatase, resorufin, amphotericin B and glucagon were acquired from Sigma-Aldrich®.

Cell culture

hnMSCs were isolated as described by Miranda et al [23] and Santos et al [24] and expanded as undifferentiated cells in α-MEM supplemented with 10 % of FBS (growing medium). Cells were passed every 2-3 days, when a 70-80 % confluence was reached. HepG2 cells (purchased from ATCC (HB-8065; American Type Culture Collection (ATCC) were cultured in α-MEM supplemented with 10 % FBS, 1 mM of sodium pyruvate and 1 % NEAA. Cryopreserved human primary hepatocytes (hpHeps; pool of 10 donors) were purchased from Invitrogen™ (HEP10, A12176), thawed on cryopreserved hepatocyte recovery medium (CHRM; CM7000, Invitrogen™) and manipulated according to manufacturer instructions. Rat primary hepatocytes (rpHeps) were isolated from Wistar rats 3- to 6-month old, weighting 200 to 400 g, obtained from Charles River Laboratories and cultured according to Miranda et al [25]. Prior to each experiment, the animals were kept in a separate cage for at least 24 hours, with ad libitum access to food and water. All applicable institutional and governmental regulations concerning the ethical use of animals were followed. Cell cultures of hnMSCs, HepG2, hpHeps and freshly isolated rpHeps were maintained at 37 °C in a humidified atmosphere with 5 % CO2 in air. Cell viability was assessed through trypan blue exclusion method.

Collagen Coating

Rat-tail collagen and commercial rat-tail collagen were used in this work. The protocol for rat-tail extraction was based on Rajan et al [26]. The extracted rat-tail collagen was dissolved in 0.1 % acetic acid to a stock concentration of 1 mg/mL. The stock solution was diluted in PBS to 0.2 mg/mL in a volume that assures total culture surface coverage. After 1-hour incubation at 37 ºC, cell culture surfaces were washed with PBS before inoculation. The differentiation process occurred using this collagen coating until day 17 and onwards for energy metabolism studies in well plates. Coating with commercial type I collagen was used for the microfluidic device and in parallel for the cover glasses (VWR®) in 24-well plates. Rat-tail type I commercial collagen at a stock concentration of 3 mg/mL was diluted in 0.1 % acetic acid to a final concentration of 0.2 mg/mL. This collagen was used from day 17 onwards. Coating was performed with three overnights to guarantee a good cell adhesion. The device and the well-plates were washed three times with PBS and before inoculation, the microfluidic device is washed three times with warmed IMDM and was left at the incubator for medium equilibration.

Hepatocyte Differentiation Protocol

The differentiation protocol was based in Cipriano et al [20,22]. hnMSCs were seeded at a density of $1.5x10^4$ cells/cm2, coated with rat-tail collagen, reaching a cell confluency of 90 % within 24 hours after inoculation. A three-step differentiation protocol was applied using IMDM with 1 % penicillin-streptomycin-amphotericin B (P/S/A) as basal medium (BM). Briefly, the first step consisted in a 48-hour incubation of BM with 2 % FBS, 10 ng/mL of EGF and 4 ng/mL of FGF-2, for endoderm commitment and foregut induction. In the second step, cells were maintained for 10 days in BM supplemented with 10 ng/mL of FGF-4, 4 ng/mL of FGF-2, 20 ng/mL of HGF, 1 % ITS and 0.61 g/L of nicotinamide, to induce hepatoblast and liver bud formation. At day 10 of differentiation (D10), 1 % DMSO was added. In the third step, at D13, BM was supplemented with 8 ng/mL of OSM, 1 µM of dexamethasone, 1% DMSO and 1 % ITS, defined as differentiation medium (DM). At D17, as a proliferative step, cells were trypsinized, re-inoculated and maintained in this culture medium supplemented with 20 µM of 5-AZA. At D21, cells could be maintained in DM or changed to maintenance medium (MM), which is BM supplemented with 8 ng/mL of OSM, 100 nM of dexamethasone, 1 % DMSO, 1 nM of insulin and 0.2 % Bovine Serum Albumin (BSA). HLCs culture was maintained up to D34.

HLCs Response to Insulin/Glucagon Stimuli

The hormone stimuli assays were performed at D34, as described in Correia et al [27]. In the insulin stimuli, a 2-hour exposure to starvation medium (SM: DMEM, 1% P/S, 4 mM of Glutamine, 1 % DMSO, 8 ng/mL of OSM and 0.2 % BSA) was performed followed by an 8h-incubation with 80 nM of insulin in SM. Negative control was performed in parallel in which cells were maintained in SM. In the glucagon stimuli, an 8-hour exposure to 100 nM of glucagon in SM was performed. Negative control was performed in parallel in which cells were maintained in SM.

Microfluidic Device Operation

Set up. The device herein used was the Xona Microfluidics Standard Neuron Device (SND150) with a 150 µm microgroove barrier. The cover glasses (VWR®) used for plasma bonding were firstly submitted to cleaning procedure consisting on sonication in a water bath for 30 minutes, being rinsed in distilled water, followed by rinsing in 70 % ethanol and three times rinsing in distilled water. As a sterilization procedure, the cover glasses were allowed to dry in a laminar flow hood cabinet, under UV light exposure. The next step was to place both the microfluidic device and the cover glass into a Plasma Cleaner (Harrick Plasma) for plasma bonding procedure, for about 1 minute, at 300 mTorr. The channels were filled with 70 % ethanol until the device was used. A cleaned glass slide was placed on top of the chambers to avoid liquid evaporation. The devices were stored at 4º C, up to 5 months. Before use, the microfluidic channels were washed with water to remove the ethanol.

HLCs inoculation. At D17 of differentiation, a suspension containing $7.5x10^4$ cells was centrifuged, at 200x*g* for 5 minutes, and resuspended in 10 µL of DM containing 20 % FBS, in order to inoculate one microfluidic channel. After 1 hour, when most of the cells were adherent, 100 µL of the same DM was added to each one of the four wells to allow further cell adhesion. Up to 1 hour later, 200 µL of DM without FBS containing 20 µM 5-AZA, as a proliferative step, was added to each one of the wells. In parallel, 24-well plates were inoculated at a seeding density of 30 000 cells/cm^2.

Quantitative Real-Time Polymerase Chain Reaction (qRT-PCR)

Total RNA was isolated from samples with 0.15-1.0 million of cells using Trizol® (Life Technologies) and extraction was performed according to manufacturer instructions and quantified by measuring absorbance at 260 nm using LVis Plate mode (SPECTROstar Omega, BMG Labtech, Ortengerg, Germany). 260/280 nm and 230/280 nm ratios were used as purity measurements for protein and solvent presence, respectively, considering ratios between 1.8-2.2. cDNA was synthesized from 0.5-1 µg RNA using NZY First-Strand cDNA Synthesis kit (NZYTech) according to the manufacturer instructions. Quantitative real time PCR was performed using PowerUp™ SYBR® Green Master Mix (Life Technologies) was prepared for a final reaction volume of 15 µL, using 2 µL of template cDNA and 0.333 µM of forward and reverse primers. Table 1 (Appendix) presents the specific primers in this work. The reaction was performed on 7300 Real-Time PCR System (Applied Biosystems®/ Life Technologies) consisting of a denaturation step at 95 °C for 10 minutes, 40 cycles of denaturation at 95 °C for 15 seconds, annealing at 60 °C for 1 minute and extension at 72 °C for 30 seconds. A dissociation stage was added to determine the melting temperature (Tm) of a single nucleic acid target sequence as a quality and specificity measure. The comparative Ct method ($2^{-\Delta\Delta Ct}$) was used to quantify gene expression, which was normalized to a reference gene (β-actin).

Periodic Acid Schiff's (PAS) Staining

Cultured cells were washed with PBS and fixed with 4 % paraformaldehyde (PFA; Sigma-Aldrich®) in PBS at room temperature (RT), for 15 minutes. One sample was incubated with amylase for 15 minutes at 37º C allowing to distinguish between positive and unspecific staining since it digests glycogen. Cell surface was oxidized with 1 % Periodic Acid (Sigma-Aldrich®) in water for 10 minutes. A washing step with distilled water for 5 minutes was followed by incubation with Schiff's reagent for 15 minutes. Cells were washed again and counterstained with Mayers' Hematoxylin (Sigma-Aldrich®). The wells were rinsed with distilled water and were observed under light microscope (Olympus CK30 inverted microscopy).

Immunocytochemistry

For immunocytochemistry staining adherent cells were, firstly, washed with PBS and fixed with 4 % PFA and 4 % sucrose in PBS, at RT, for 15 minutes. The next step was permeabilization cells with 0.3 % Triton-100 in PBS, for 15 minutes at RT. Afterwards, blocking buffer containing 2.5 % BSA, 2 % FBS in PBS was applied for 30 minutes at RT. Incubation with primary antibody was carried out at 4ºC overnight. The following primary antibodies were used: CK-18 (Santa Cruz Biotechnology®), organic anion-transporting polypeptide-C (OATP-C; Santa Cruz Biotechnology®), multidrug resistance protein-2 (MRP-2; Santa Cruz Biotechnology®), albumin (ALB; Cruz Biotechnology®) and HNF-4α (Perseus Proteomics Inc.). 1h-incubation with secondary antibody was performed at RT. The final step was to apply DAPI (Sigma-Aldrich®) and aqua-poly/mount coverslipping medium (Polysciences). The coverslides were observed on an inverted fluorescence microscope (Axiovert 200M, Carl Zeiss) coupled with a monochrome camera (AxioCam MNC, Carl Zeiss). Sample fluorescence was examined in fluorescence at excitation/emission wavelengths of 590/617 nm (goat anti-rabbit Alexa Fluor 594; Life Technologies), 495/519 nm (donkey anti-mouse Alexa Fluor 488; Life Technologies) and 358/461 (DAPI). Images were acquired using AxioVision Rel. 4.7 software.

Urea and Albumin Quantification

Urea and albumin were quantified in cell culture supernatants using a colorimetric urea kit (QuantiChrom™ Urea Assay Kit, DIUR-500, BioAssay Systems) and ELISA commercial kit (ICL's Human Albumin ELISA kit), respectively. The absorbance was measured at 520 nm for urea and 450 nm for albumin ELISA in a microplate reader (SPECTROStar Omega, BMG Labtech), according to manufacturer's instructions. Data is presented as the rate of production: $\mu g/10^6$ cells.h (for urea) and $pg/10^6$ cells.h (for albumin).

Biotransformation Activity

Phase I metabolism reactions were assessed by quantification of 7-ethoxyresorufin-O-deethylase (EROD) activity and 7-ethoxycoumarin-O-deethylase (ECOD) activity. Phase II metabolism reactions were quantified by measuring UGTs activities. EROD assay

allows to assess human CYP1A1 and CYP1A2 [28] activity. The protocol was adapted from Donato et al [29] and consisted in a 90 minutes' cell incubation with IMDM containing 8 µM 7-ethoxyresorufin followed by a 2-hour enzymatic digestion with β-Glucuronidase/Arylsulfatase. The concentration of the product (7-hydroxyresorufin) was measured at an excitation wavelength of 530 nm and an emission of 590 nm. ECOD activity reflects human CYP2B6, 1A2 and 2E1 activity [28,30]. The protocol consisted on a 90 minutes' cell incubation with 0.8 mM 7-ethoxycoumarin diluted in IMDM. After 2-hour enzymatic digestion with β-Glucuronidase/Arylsulfatase, liquid-liquid extractions, with chloroform (collecting the organic phase) and a solution of 1.0 M NaCl and 0.1 M NaOH (collecting the aqueous alkaline phase), the concentration of the product (7-hydroxycoumarin) was measured at an excitation wavelength of 340 nm and an emission wavelength of 460 nm. UGTs activity was determined by cell incubation with 4-methylumbelliferone (4-MU). The substrate was quantified either before and after cell incubation, in order to evaluate the extent of conversion. The protocol was based on Miranda et al. [30]. Briefly, a 1-hour cell incubation with 100 µM 4-MU solution diluted in HBSS was performed. Afterwards, the supernatant was transferred into a 96-well plate and 4 µL of NaOH at 0.1 M was added per well in order to achieve pH = 11. The fluorescence was measured at an excitation wavelength of 340 nm and an emission wavelength of 460 nm.

Protein Quantification

Protein concentration was determined by measuring the absorbance at 280 nm, using LVis plate mode (SPECTROstar Omega, BMG Labtech). Total protein was quantified after cell lysis with 0.1 N NaOH solution at 37°C overnight and stored at -20ºC for further analysis.

Statistical Analysis

The results are given as the Average ± SEM. Statistical data analysis was performed using PRISM 6.0 (GraphPad Software), using a two-way ANOVA with Tukey's test. $p < 0.05$ was considered statistically significant.

II. Results and Discussion

HLCs could be adapted to rat-tail type I commercial collagen coated surfaces

With the ultimate goal of adapting HLCs to a microfluidic device, the surface coating was firstly optimized. Our group has previously optimized a differentiation protocol for deriving HLCs from hnMSCs and characterized them at a morphological, biochemical and biotransformation level [20,22]. However, the collagen coating used in that protocol did not enable a homogeneous cell inoculation in the microfluidic device due to the formation of gel clogs in the channels. Therefore, a step of coating with commercial collagen was attempted. HLCs seeded in 0.2 mg /mL of commercial collagen diluted in acetic acid provided better morphology, maintaining its adherence until D34 (data not shown). Therefore, this coating was used for further studies of maintenance of HLCs' characteristics namely, biotransformation activity, glycogen storage ability and immunocytochemical staining.

Different dexamethasone and insulin concentrations do not affect HLCs' biotransformation capacity

Our protocol for deriving and culturing HLCs [20,22] consists on the use of DM that contains high concentrations of dexamethasone (1 µM) and insulin (1.72 µM). However, glucocorticoids may cause insulin resistance [31] and, therefore, interfere with cell energy metabolism. Thus, there was the need to change the medium formulation to closer physiological concentrations by decreasing dexamethasone and insulin concentrations to 100 nM and 1 nM, respectively (MM), as described by Estal et al in the culture of primary mouse hepatocytes [32].

The influence of the alterations regarding media and collagen coating was evaluated on the HLCs' phenotype, glycogen storage ability, presence of hepatic markers and biotransformation activity. These assays were performed in HLCs cultured in coated coverslips since HLCs in the MD would also be in contact with a coated glass surface. D27 and D34 were chosen as time points for these evaluations because D27 is considered to be the day at which the differentiation process ends [20]; whereas D34 represents maintenance of cells in culture for one week long.

We observed that in both MM and DM conditions HLCs presented binucleated cells and a polygonal shape throughout time in culture and displayed glycogen storage ability (data not shown) and the presence of specific hepatic markers such as HNF-4α, ALB, the influx transporter OATP-C, the efflux transporter MRP-2 and CK-18 (Figure 2), at D27 and D34, suggesting the maintenance of hepatic phenotype in culture.

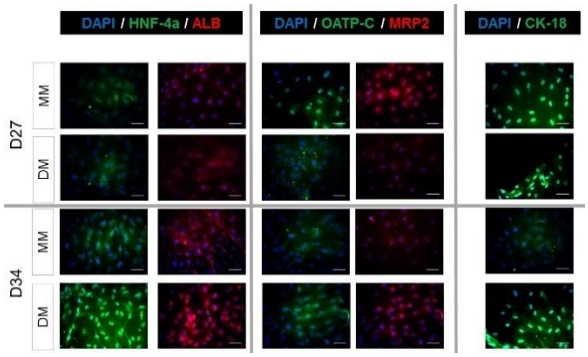

Figure 2 - Immunocytochemical staining revealed the presence of specific hepatic markers: HNF-4α, ALB, OATP-C, MRP2 and CK-18 in HLCs maintained in both media, at D27 and D34. Cell nuclei were counterstained with DAPI. Scale bar = 50 µm.

To assess the effect of the media culture on HLCs' biotransformation competence, EROD, ECOD and UGTs activities were also tested. hnMSCs were used as a negative control while HepG2, rat primary hepatocytes and human hepatocytes were used as positive controls. EROD activity (Figure 3 a), covering CYP1A1/2, showed a slight increase from D27 to D34, in cells maintained in both MM and DM, although not significant ($p > 0.05$). HLCs in MM, which has lower dexamethasone presented higher EROD activity in both days (non-significant) than HLCs in DM. In fact, dexamethasone was shown to decrease CYP1A1 activity in adult human hepatocytes [33]. In contrast, ECOD assay, covering CYP2B6/1A2/2E1 activities, showed a slight decrease in activity from D27 to D34 (non-significant) in both media (Figure 3 b). At D34, the activity was slightly higher in HLCs maintained in DM (non-significant). Indeed, dexamethasone is a known inducer of CYP2B6 [34] in human hepatocytes. Herein, UGTs activity was evaluated since most phase II reactions within the human body are catalysed by these enzymes [35]. UGTs activity in HLCs showed no significant differences when compared to human hepatocytes ($p > 0.05$) in all tested conditions, being always higher than all other controls (Figure

3 c). Thus, HLCs maintained its competence throughout culture time under the different culture media formulations.

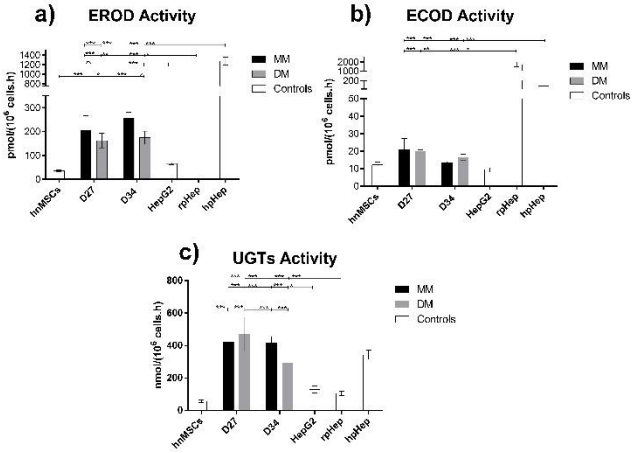

Figure 3 - Effect of culture time and medium composition on Phase I activity and Phase II activity: a) EROD b) ECOD activities and c) UGTs activity. Data is represented as Average ± SEM (n=2-4). Undifferentiated hnMSCs and HepG2 cell line, rpHeps and cryopreserved hpHep are negative and positive controls, respectively (white bars). *, **, *** Significantly differs among the controls with $p < 0.05$, $p < 0.01$ and $p < 0.001$, respectively.

Different dexamethasone and insulin concentrations induce altered gene expression profiles in HLCs

DM and MM have both equal glucose concentrations (25 mM) but the ratios of insulin to dexamethasone are 1.72 in DM and 0.01 in MM. Therefore, in DM the insulin effect may overlap dexamethasone effect while the opposite happens in MM. We studied the gene expression profile of HLCs cultured in MM and DM, in plates, at different culture time points (D27 and D34) using as a reference HLCs subjected to 8h-fasting at D34 since this condition has lower glucose concentration (5 mM) and has no dexamethasone or insulin (Figure 4).

HLCs in DM showed an increased gene expression, except for *GLUT1* and *ERRA*, from D27 to D34, indicating higher HLCs maturation probably due to the dexamethasone and insulin concentrations [36] used in the differentiation protocol, (Figure 4 a and e). Indeed, glucose transporter *GLUT1* expression decreased from D27 to D34 in both MM and DM (only significant in DM). This may be explained due to a transition from a foetal phenotype, which presents higher *GLUT1* expression, to a neonatal phenotype, having little expression in neonatal and adult hepatocytes [37]. *ERRA* gene regulates the transition from glycolysis to fatty acid oxidation [38]. Possibly, the decrease in its expression is related to a continued exposure to high concentrations of insulin, which induces glycolysis and inhibits fatty acid oxidation [4].

In contrast, when exposed to MM the expression levels of *PEPCK*, *G6PASE*, *ACOX1*, *FXR* and *NRF1* presented the opposite trend being higher at D27 (Figure 4 b, c, d and e).

Overall, DM enhanced HLCs' metabolic characteristics during culture time, from D27 to D34. However, for the purpose of studying cells adaption to fasting and/or the response to insulin and glucagon exposure, a lower gene expression profile, as the one observed in HLCs in MM is needed.

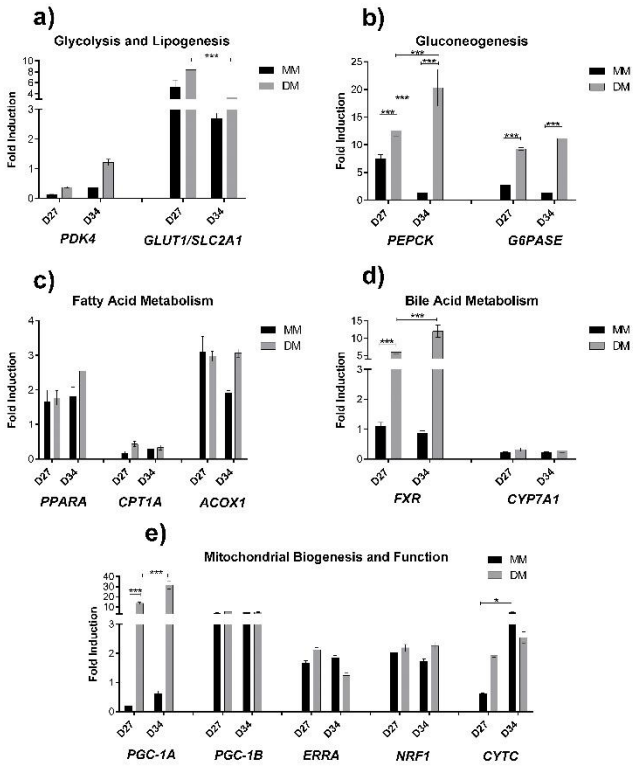

Figure 4 - Gene expression in HLCs throughout culture time in MM and DM regarding a) glycolysis and lipogenesis; b) gluconeogenesis; c) fatty acid metabolism; d) bile acid metabolism and e) mitochondrial biogenesis and function. The graphs represent HLCs' evolution in MM and DM relative to 8h-fasting at D34. Data is represented as Average ± SEM (n=2-6). *, **, *** Significantly differs from the different media composition and the days of differentiation with $p < 0.05$, $p < 0.01$ and $p < 0.001$, respectively.

HLCs adapt their response to fasting

Energy metabolism studies were performed in HLCs at D34 given that the metabolic responses at D34 were closer to expected (data not shown). The adaption of HLCs to fasting was evaluated by the expression profile of specific genes upon 8 and 10 hours of starvation. Analysis was performed relative to HLCs cultured in MM at D34 in order to study the effect of 25 mM of glucose (in the MM) and 5 mM of glucose (in the SM).

Glucose oxidation through glycolysis is downregulated during starvation. In our experimental conditions, 8 hours of fasting presented higher expression of *PDK4* than 10 hours of fasting ($p < 0.001$) (Figure 5 a), which may be explained by a time course of events leading to glucose homeostasis. In fact, in an *in vivo* study by Palou et al, fasting rat revealed a peak in *PDK4* expression at 8 hours of fasting, showing a subsequent decrease [39]. Moreover, *SREBP-1C* and *CHREBP1* induce lipogenesis [4] and upon fasting, they were strongly downregulated. This is expected since starvation does not induce energy storage. In addition, glucose activates *CHREBP1* transcription [40] and in the condition herein evaluated, this substrate is lacking. *GLUT1* was shown to be upregulated in rat hepatocytes in both fasting and diabetes [41]. However, in HLCs, *GLUT1* was downregulated after 8 hours and maintained its expression, relative to MM, after 10 hours of fasting (Figure 5 a), suggesting that the expected gene upregulation might be seen if HLCs were submitted to a longer fasting period.

Upon starvation, gluconeogenesis is activated [4]. As expected, *PEPCK* was markedly induced ($p < 0.05$) after 10 hours of fasting (Figure 5 b). *G6PASE* approximately maintained its expression after 10 hours of fasting (Figure 5 b).

Alternatively to gluconeogenesis, *PDK4* upregulation [42] can also activate fatty acids utilization [5] inducing *PPARA*. In HLCs, *PPARA* and *ACOX1* were not induced upon starvation (Figure 5 c), but instead a decrease from 8 to 10 hours of fasting was observed. In contrast, *CPT1A* as a target of *PPARA* [4] was progressively induced with increasing duration of fasting (Figure 5 c). A similar trend was observed in fasting rats where *CPT1A* expression increased from 8 to 24 hours of fasting [39]. In addition, in the same study, *PPARA* expression had a peak after 4 hours, decreasing afterwards while *ACOX1* presented an increasing trend [39]. The trend of *ACOX1* expression in rat livers and in HLCs was contrasting. Thus, it would be interesting to evaluate other time points of starvation.

PGC-1A (mitochondrial biogenesis) was upregulated upon 10 hours of starvation when compared to 8 hours of starvation ($p < 0.01$) (Figure 5 e). Such effect is in line with previously reported in mice [10]. PGC-1α induces gluconeogenesis and β oxidation. Upon starvation, HLCs showed an activation of both pathways, more relevant in gluconeogenesis, through upregulation of *PEPCK*. In fact, *CYP7A1* was also upregulated in fasting ($p < 0.05$) (Figure 5 d), which may be related to PGC-1A activation [43]. Our results are in accordance with the reported *CYP7A1* activation in livers of fasted mice [43], augmenting the synthesis of bile acids. *PGC-1A* upregulation upon fasting may influence *CYP7A1* expression. Contrary to reported [17,18], *FXR* was not induced by PGC-1α in HLCs (Figure 5 d), upon fasting. FXR senses bile acids and between 8 and 10 hours of fasting, bile acid synthesis was induced through *CYP7A1* activation. Nevertheless, beyond a certain pool size of bile acids, their synthesis is inhibited due to cytotoxic effects [13]. Thus, a longer fasting time could result in *FXR* upregulation. PGC-1β is related to lipogenesis [44] and our results for HLCs showed a downregulation of this gene after 8 hours of fasting ($p < 0.05$), followed by an increase in expression ($p < 0.05$) (Figure 5 e). Upon fasting, there is a lack of substrates to be used in this pathway, thus explaining the observed downregulation. Due to its widespread tissue distribution, PGC-1β may fulfil other functions necessary for the basal cell energy requirements and these results may not be fully explained just by the response to fasting [45]. Estrogen-related receptor α (ERRα) is a nuclear receptor related with mitochondrial function [46]. ERRα interacts with *PEPCK* promoter, thus inhibiting gluconeogenesis [46]. Herein, *ERRA* was downregulated (non-significant), presenting approximately the same level of expression, after 8 and 10 hours of fasting (Figure 5 e). This downregulation accompanied by an induction of gluconeogenesis in HLCs, possibly suggests that ERRα was not activated in order to gluconeogenesis occur. In addition, ERRα is reported to induce expression of genes related to mitochondrial biogenesis, such as nuclear respiratory factor 1 (*NRF1*), and respiratory chain cytochrome C (*CYTC*) [46]. Not much is known about the metabolic regulation of these two genes, nevertheless, *NRF1* and *CYTC* were downregulated upon fasting in HLCs (non-significant) (Figure 5 e), possibly due to the lack of induction of ERRα.

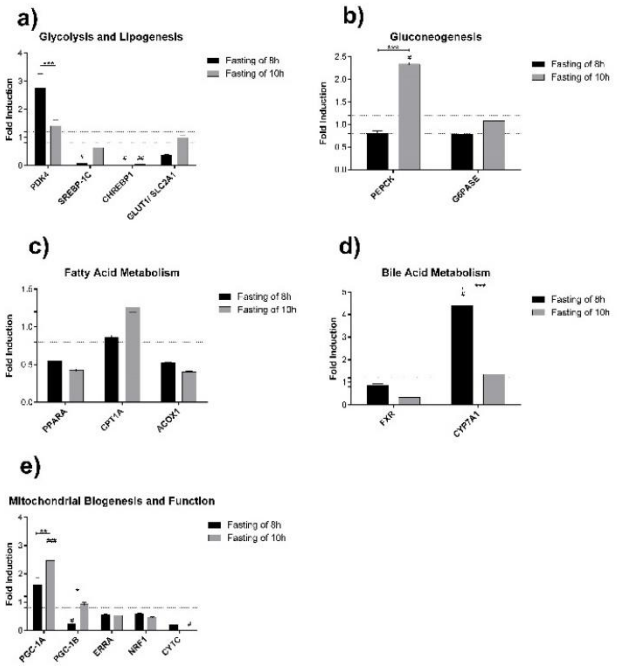

Figure 5 - HLCs' adaptive response to fasting at D34. Expression of specific genes of a) glycolysis and lipogenesis, b) gluconeogenesis, c) fatty acid metabolism, d) bile acid metabolism and e) mitochondrial biogenesis and function. The graphs represent the fold induction of HLCs in response to 8h- and 10-fasting relative to MM. Grid lines represent fold induction equal to 0.8 and 1.2. Data is represented as Average ± SEM (n=2-6). *, **, *** Significantly differs from the different media composition and the days of differentiation with $p < 0.05$, $p < 0.01$ and $p < 0.001$, respectively. #, ##, ### Significantly induced or repressed expression with $p < 0.05$, $p < 0.01$ and $p < 0.001$, respectively.

Based on these results, we observed that all the genes tested regarding glycolysis, gluconeogenesis, bile acid metabolism and mitochondrial function respond as expected, except for *G6PASE*, although showing the expected increasing trend, and *FXR*. We could conclude that the pathway that most responded to starvation in HLCs was gluconeogenesis which is actually the first pathway to respond to fasting [47]. Indeed, during the gestation period of several animals, including humans, the mother, in a well-fed state, provides glucose and the foetus does not have the need of producing it. However, fasting mothers can induce premature foetal gluconeogenesis [48], showing that this pathway is an early event in development. Genes related to fatty acid metabolism may not present the expected physiological responses, because we only considered 8 and 10 hours of fasting. Metabolic pathways are regulated by a cascade of events occurring in different time points. For genes involved in gluconeogenesis regulation, this window of time is adequate whereas fatty acid metabolism and bile acid metabolism may demand earlier and later time points, respectively.

HLCs respond to insulin and glucagon exposure

In addition to adapt their functions to starvation, hepatocytes are expected to stimulate or inhibit genes controlling glucose metabolism when exposed to insulin or glucagon. Therefore, HLCs response to insulin or glucagon stimuli was evaluated under low glucose concentrations (5 mM glucose) in cells that were maintained in MM. Human primary hepatocytes maintained in the same culture conditions were used as controls.

Insulin stimulates glycolysis and lipogenesis [4] and both

HLCs and human hepatocytes when incubated with insulin, inhibited *PDK4* expression (Figure 6 a), indicating increased pyruvate consumption and glycolysis, although only significant in HLCs ($p < 0.001$). The opposite response was observed when cells were exposed to glucagon (Figure 6 a). On the other hand, *CHREBP* (lipogenesis pathway) and *GLUT1* (glycolysis pathway) were downregulated in response to insulin ($p < 0.05$ and $p < 0.001$, respectively) while *GLUT1* was upregulated in response to glucagon ($p < 0.001$) in HLCs (Figure 6 a). Moreover, *SREBP-1C* was downregulated ($p < 0.05$) in the positive control. This gene is activated when senses elevated cholesterol concentration [49], which was not present in the medium. In addition, insulin stimulation in rat hepatocytes with a duration of 6 hours increased *SREBP-1C* expression [50], suggesting that a shorter period of insulin incubation would be interesting to study. ChREBP, on the other hand, is indirectly activated by insulin since insulin induces lipogenesis. *CHREBP* was upregulated in primary hepatocytes and downregulated in HLCs ($p < 0.05$) (Figure 6 a) but other mechanisms may induce synergistically the expression of *CHREBP* towards lipogenesis. Finally, the hepatic-specific glucose transporter *GLUT2* was only detected in primary hepatocytes.

Moreover, as expected, *PEPCK* and *G6PASE* were upregulated when medium contained glucagon and downregulated in response to insulin, in both HLCs and primary hepatocytes (Figure 6 b), activating gluconeogenesis in order to produce glucose for extrahepatic tissues [4].

The oxidation of fatty acids is downregulated by insulin and stimulated by glucagon [11] to obtain energy and PPARα promotes β oxidation [4]. Longuet et al reported that glucagon signalling activates a PPARα-dependent cascade of events, enhancing fatty acid oxidation in mice [11]. PPARα targets *ACOX1*, the rate-limiting enzyme of the partial oxidation of fatty acids in peroxisomes and *CPT1A* [51]. *PPARA* was downregulated, in HLCs, in response to insulin ($p < 0.05$) upregulated upon glucagon treatment in HLCs and human hepatocytes (non-significant) (Figure 7 a). However, in HLCs just *PPARA* was upregulated while target genes of PPARα did not show different responses to insulin or glucagon (Figure 7 a). This may indicate that this pathway is not fully developed in HLCs. In fact, hepatocytes isolated from guinea pig were able to oxidize fatty acids only 12 hours after birth [52]. The lack of fatty acids in the medium could also be the reason why the genes related to fatty acids metabolism do not present the expected expression.

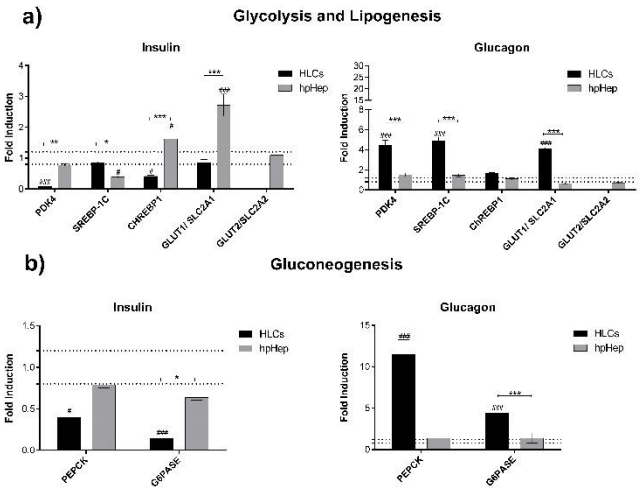

Figure 6 – Gene expression in HLCs in response to insulin and glucagon regarding a) glycolysis and lipogenesis and b) gluconeogenesis. Grid lines represent fold induction equal to 0.8 and 1.2. Data is represented as Average ± SEM (n=2-6). *, **, *** Significantly differs from the different media composition and the days of differentiation with $p < 0.05$, $p < 0.01$ and $p < 0.001$, respectively. #, ##, ### Significantly induced or repressed expression with $p < 0.05$, $p < 0.01$ and $p < 0.001$, respectively.

Regarding bile acids metabolism, insulin resulted in downregulation of *FXR* in both HLCs ($p < 0.05$) and human hepatocytes (non-significant) while glucagon resulted in its upregulation (non-significant) (Figure 7 b). The downregulation of *FXR* induced by insulin is in line with previously reported in rat hepatocytes cultured in low glucose concentrations (5 mM) [53]. Since *FXR* was downregulated by insulin, we may infer that the expression of its target [53], small heterodimer partner (*SHP*), will not be induced, as observed (Figure 7 b). *CYP7A1* was also downregulated in HLCs ($p < 0.01$) and primary hepatocytes ($p < 0.05$) during prolonged exposure to insulin (Figure 7 b), which is in accordance with previous observations [16]. However, *SHP* and *CYP7A1* expression had no differences when cells were incubated with glucagon. FXR positively regulates bile salt export pump (BSEP), excreting bile acids from the hepatocytes into bile canaliculus [14]. *BSEP* was downregulated when human hepatocytes were exposed to insulin and glucagon (Figure 7 b). However, in HLCs, *BSEP* was upregulated in response to glucagon, possibly due to induction by FXR. We infer that the expected responses were not observed may be due to the lack of cholesterol and bile acids in the medium [54]. Several papers suggest that *FXR* upregulation occurs through the action of PGC-1α upon fasting [17,18]. However, in HLCs, *FXR* was upregulated by glucagon but it was downregulated when HLCs were in fasting conditions (Figure 5 d).

PGC-1α (mitochondrial biogenesis) co-activates genes regarding gluconeogenesis (*PEPCK* and *G6PASE*) [3,55]. In both HLCs and hepatocytes, glucagon treatment caused *PGC-1A* upregulation whereas insulin repressed it ($p < 0.05$) (Figure 7 c). PGC-1β, on the other hand, is related to lipogenesis, among other mitochondrial functions [44]. In response to insulin, both HLCs ($p < 0.01$) and hepatocytes ($p < 0.001$) presented *PGC-1B* upregulation (Figure 7 c). The physiological response of PGC-1β to hormonal signaling has not yet been clarified. However, since insulin also induces lipogenesis, this may be the expected response. Glucagon caused a decrease in the

upregulation of *PGC-1B* (Figure 7 c), which would be a possible response since lipogenesis is repressed by glucagon [11]. *ERRA*, *NRF1* and *CYTC* were mostly downregulated by insulin (Figure 7 c). ERRα was shown to repress gluconeogenesis [56], which might explain the strong repression shown by human hepatocytes. In HLCs, *ERRA* essentially presented the same level of expression in response to glucagon and insulin (Figure 7 c). Glucagon mostly induced an increase in expression of these genes when compared to insulin. PGC-1α was reported to have stimulatory effects in ERRα, Nrf1 and CytC [57]. Therefore, the trend presented in gene expression may reveal a possible upregulation if the incubation time with glucagon would be longer. The response of this set of genes to glucagon contrasts with their response to fasting (Figure 5 e). Thus, it is difficult to conclude what would occur in a physiological context.

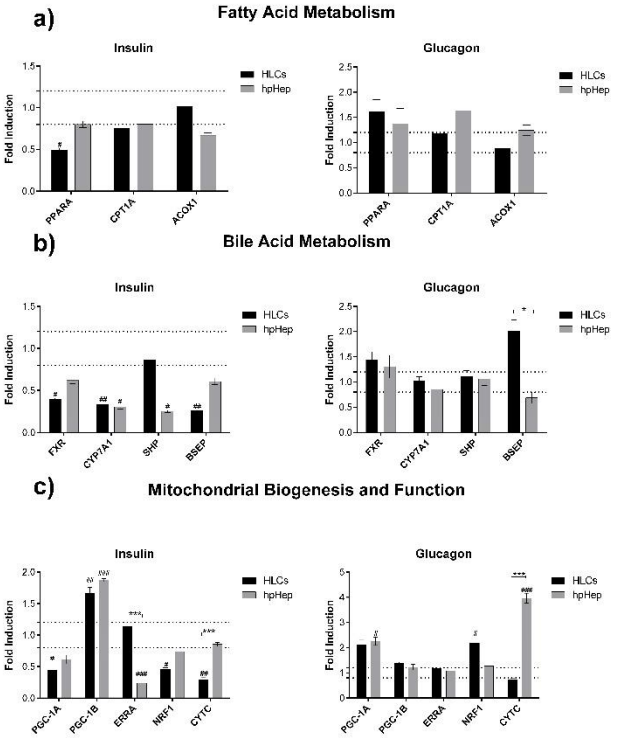

Figure 7 – Gene expression in HLCs in response to insulin and glucagon regarding a) fatty acid metabolism, b) bile acid metabolism and c) mitochondrial biogenesis and function. Grid lines represent fold induction equal to 0.8 and 1.2. *, **, *** Significantly differs from the different media composition and the days of differentiation with $p < 0.05$, $p < 0.01$ and $p < 0.001$, respectively. #, ##, ### Significantly induced or repressed expression with $p < 0.05$, $p < 0.01$ and $p < 0.001$, respectively.

In sum, gluconeogenesis is the pathway where HLCs presented more accentuated and expected responses. Glucose is a medium component present in high concentrations during all the differentiation process. Therefore, this biomolecule possibly stimulates pathways that regulate its use. *PDK4*, which is related to glycolysis, also showed significant downregulation and upregulation when HLCs were exposed to insulin and glucagon, respectively. Considering fatty acid oxidation, in HLCs, genes downstream to *PPARA* may show an upregulating trend if the exposure to glucagon was prolonged. Genes regarding bile acid metabolism responded to insulin stimuli but did not show significant responses to glucagon, suggesting the need for optimization of hormone concentration or time incubation. PGC-1α induces gluconeogenesis gene expression and interacts with PPARα, activating fatty acid oxidation [58] and is a co-activator of FXR, inhibiting bile acid synthesis. Our results showed that when *PGC-1A* was upregulated, these genes were also. Godoy et al demonstrated that including bile salts in hepatocytes culture increased expression of mature liver function genes [54]. Thus, it would be interesting to use a medium containing biomolecules frequently in contact with hepatocytes such as fatty acids, cholesterol and bile acids and adapt their concentration to the one found in the fasted and fed states. Incubation with these compounds might produce responses, possibly closer to an *in vivo* situation.

HLCs can be maintained up to two weeks in the microfluidic device

The results obtained above demonstrated a dual effect of MM and DM in HLCs' culture. MM enables the observation of responses related to energy metabolism homeostasis, by lowering gene expression, while DM induces a more mature phenotype in HLCs. In addition, HLCs were responsive to insulin and glucagon and adapted their metabolism to fasting, demonstrating their competence for energetic metabolism studies. Moreover, HLCs cultured in coverslips coated with commercial collagen maintained its phenotype, biotransformation activity, glycogen storage ability and presence of hepatic markers throughout time in culture. Therefore, we proceeded to adapt HLCs to the microfluidic device (MD). HLCs were inoculated at D17, acquiring a polygonal shape after 1 hour (data not shown). Their morphology was maintained throughout culture time (Figure 8).

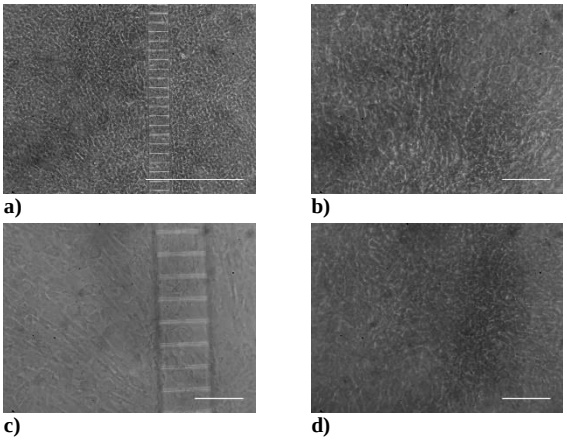

Figure 8 - HLCs morphology at D17 and the change from a fibroblast-like shape to a polygonal shape throughout the day of inoculation, in the MD: a) HLCs before tripsinization (scale bar = 500 µm); b) HLCs 20 minutes after device inoculation (scale bar = 500 µm); c) HLCs 1 hour after device inoculation (scale bar = 500 µm); d) HLCs 2 hours after device inoculation (scale bar = 100 µm).

Urea and albumin production were quantified, not showing significant differences between both days and media composition (Figure 9) suggesting the maintenance of a hepatic phenotype in the MD.

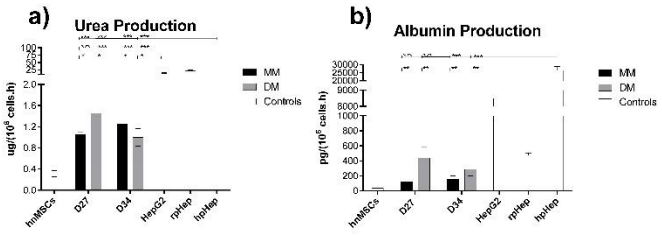

Figure 9 – Effect of culture time in HLCs cultured in the MD in MM and DM on a) urea and b) albumin production. Data is represented as Average ± SEM (n=4-5). Undifferentiated hnMSCs and HepG2 cell line, rpHeps and hpHeps are negative and positive controls, respectively (white bars). *, **, *** Significantly differs among the controls with $p < 0.05$, $p < 0.01$ and $p < 0.001$, respectively.

Gene expression profile of HLCs cultured in the MD, in MM and DM was analysed and compared to HLCs cultured in the traditional 2D static system.

HLCs cultured in MM presented higher gene expression at D27 for all genes tested while in plates, *PDK4* ($p < 0.001$), *CPT1A* ($p < 0.05$) and *PGC-1A* ($p < 0.001$) presented higher gene expression at D34 (Figure 10 a). On the other hand, *PEPCK* ($p < 0.05$), *G6PASE* ($p < 0.05$) and *PGC-1A* ($p < 0.001$) showed increased expression at D34 in HLCs cultured in DM, in this device (Figure 10 b).

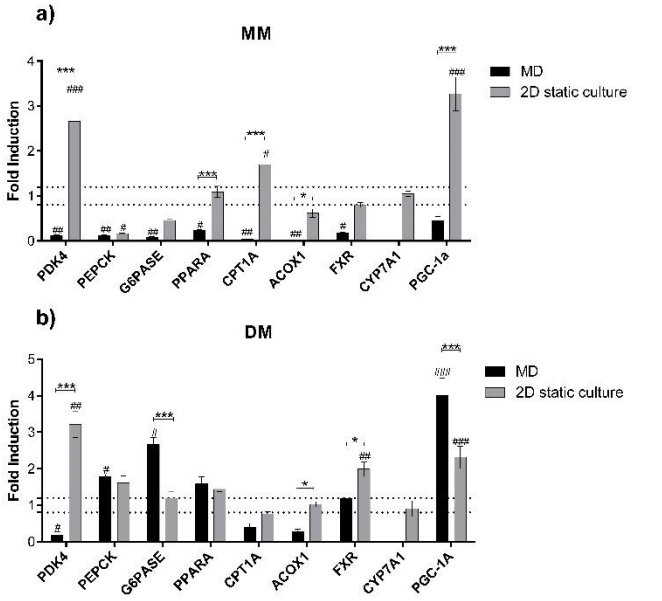

Figure 10 – Gene expression levels in HLCs cultured in MD or 2D static cultures in a) MM and b) DM. The graphs represent the fold induction of HLCs in MM and DM at D34 relative to D27. Grid lines represent fold induction equal to 0.8 and 1.2. Data is represented as Average ± SEM (n=2-4). *, **, *** Significantly differs from the different media composition and the days of differentiation with $p < 0.05$, $p < 0.01$ and $p < 0.001$, respectively. #, ##, ### Significantly induced or repressed expression with $p < 0.05$, $p < 0.01$ and $p < 0.001$, respectively.

Regarding MM, gene expression in HLCs in the device at D27 was greater in all genes tested than in plates and at D34, *PDK4*, *PEPCK*, *G6PASE* and *PGC-1A* ($p < 0.001$) continued to have greater expression in the MD (Figure 11 a).

DM at D27, on the other hand, induced greater expression in *PDK4* ($p < 0.001$), *CPT1A* and *ACOX1* in the MD. At D34, just *PDK4* and *CPT1A* had higher expression in the MD when compared to plates (Figure 11 b).

When comparing gene expression of HLCs in MM relative to DM, at D27, all the genes, except *PDK4* were upregulated in the MD (Figure 12 a). At D34, the difference between the two media was not so pronounced. However, expression of *PEPCK*, *G6PASE* and *PGC-1A* was significantly higher in the MD ($p < 0.001$) (Figure 12 b).

Overall, MM enhanced gene expression in the MD by comparison to 2D static cultures although a decrease in expression from D27 to D34 was observed but was not significant.

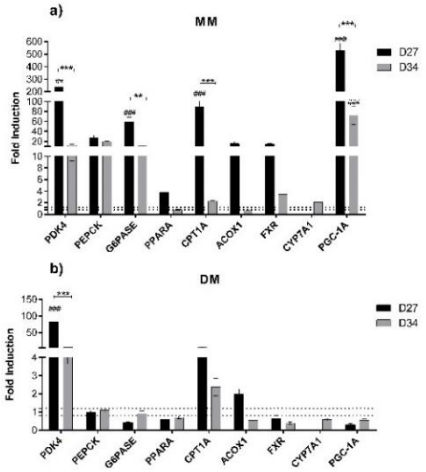

Figure 11 – Gene expression levels in HLCs (D27 and D34) cultured in a) MM and b) DM, in both days. The graphs represent the fold induction of HLCs cultured in MD relative to plates. Grid lines represent fold induction equal to 0.8 and 1.2. Data is represented as Average ± SEM (n=2-4). *, **, *** Significantly differs from the different media composition and the days of differentiation with $p < 0.05$, $p < 0.01$ and $p < 0.001$, respectively. #, ##, ### Significantly induced or repressed expression with $p < 0.05$, $p < 0.01$ and $p < 0.001$, respectively.

Concluding, there are differences regarding MD and 2D static culture systems. Opposite trends when comparing HLCs cultured (in the MD and plates) in MM or DM were observed. The differences between these two systems may be due to the inoculum and the possibility of creating a flow, by a daily addition of 30 µL of medium from the bottom wells to the upper wells in the MD.

HLCs in the MD were cultured at a higher inoculum than in plates. In fact, high density cultures (> 200 000 cells/cm^2) enhance cell function [59]. In a study performed by Zhang et al, HepG2 seeded at high densities in a microfluidic device presented greater albumin production than 2D static cultures [59]. We can infer that the decrease in concentrations of insulin and dexamethasone (in MM), which are important in the differentiation protocol, may be supplanted by increased cell-to-cell contact in the MD, mimicking the in vivo liver configuration where high density of hepatocytes is in close contact [59]. However, this trend is maintained up to D34 just for a set of genes regulating gluconeogenesis. In addition, fluid friction further approximates this culture system to liver microenvironment, since in vivo liver regeneration is related to portal pressure [60]. Furthermore, cells cultured in MD were maintained in small medium volumes, where diffusion of growth factors and secreted biomolecules is limited, surface-to-volume ratio is very high and molecular diffusion resembles what occurs physiologically [61].

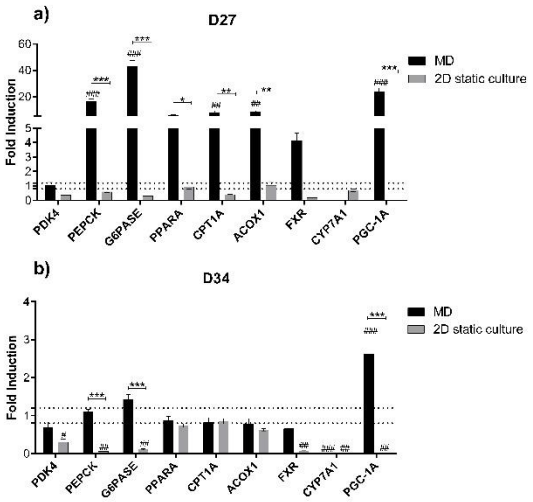

Figure 12 – Gene expression levels in HLCs cultured in MD or 2D static cultures at a) D27 and b) D34. The graphs represent the fold induction of HLCs cultured in MM relative to DM. Grid lines represent fold induction equal to 0.8 and 1.2. Data is represented as Average ± SEM (n=2-4). *, **, *** Significantly differs from the different media composition and the days of differentiation with $p < 0.05$, $p < 0.01$ and $p < 0.001$, respectively. $^{\#}$, $^{\#\#}$, $^{\#\#\#}$ Significantly induced or repressed expression with $p < 0.05$, $p < 0.01$ and $p < 0.001$, respectively.

III. Conclusion

This work demonstrates that hnMSCs-derived HLCs obtained by a specific differentiation protocol were capable of responding to insulin and to glucagon and to adapt their metabolism to fasting. Although the medium composition should be optimized in order to better mimic the composition of blood in the human body, containing additional biomolecules [54], we could successfully inoculate these cells into a MD and maintain them functional for up to two weeks. Further information regarding MD culture will be gathered once the response to fasting and to hormone signalling is evaluated in the MD culture. We hope that future studies in the context of metabolic syndrome using HLCs and other relevant cell types, in similar MDs, will be useful to create a better understanding of this pathology and thus designing therapeutic strategies.

Appendix

Name	Sequence	(TmºC)
B-actin_F	CATGTACGTTGCTATCCAGGC	87.80
B-actin_R	CTCCTTAATGTCACGCACGAT	87.80
PDK4_F	TCTGAGGCTGATGACTGGTG	80.60
PDK4_R	GGAGGAAACAAGGGTTCACA	80.60
SREBP-1c_F	TGTTTGTTAGTGGGAGGAGTG	86.20
SREBP-1c_R	GAGGTGAGAAGGGACAACTGA	86.20
ChREBP1_F	GTTCCCTCTCTCTGCTCCTTC	86.80
ChREBP1_R	CCACACACACACATCCACAC	86.80
PEPCK_F	GCTTTTCAGCATCTCCAAGGA	80.30
PEPCK_R	GCTTCAAGGCAAGGATCTCTC	80.30
G6PASE_F	CAGAGCAATCACCACCAAGC	80.30
G6PASE_R	ACATTCATTCCTTCCTCCATCC	80.30
PPARA_F	CTGTCATTCAAGCCCATCTTC	81.60
PPARA_R	TTATTTGCCACAACCCTTCC	81.60
FXR_F	AGAACCTGGAAGTGGAACC	81.60
FXR_R	CTCTGCTACCTCAGTTTCTCC	81.60
CYP7A1_R	CCAGAAGCAATGAAAGCAGC	79.30
CYP7A1_F	GGATGTTGAGGGAGGGACT	79.30
PGC-1A_F	GCTGAAGAGGCAAGAGACAGA	80.40
PGC-1A_R	AAGCACACACACCACACACA	80.40
PGC-1B_F	GATGCCAGCGACTTTGACTC	85.90
PGC-1B_R	ACCCACGTCATCTTCAGGGA	85.90
GLUT1 _F	TCTGGCATCAACGCTGTCTTC	83.00
GLUT1 _R	CGATACCGGAGCCAATGGT	83.00
GLUT2 _F	GCTGCTCAACTAATCACCATGC	80.90
GLUT2 _R	TGGTCCCAATTTTGAAAACCCC	80.90
CPT1a_F	TCCAGTTGGCTTATCGTGGTG	80.90
CPT1a_R	TCCAGAGTCCGATTGATTTTTGC	80.90
ACOX1_F	ACTCGCAGCCAGCGTTATG	81.60
ACOX1_R	AGGGTCAGCGATGCCAAAC	81.60
NRF_F	AGGAACACGGAGTGACCCAA	83.00
NRF_R	TATGCTCGGTGTAAGTAGCCA	83.00
ERRA_F	AGGGTTCCTCGGAGACAGAG	71.60
ERRA_R	TCACAGGATGCCACACCATAG	71.60
CYTC_F	CTGATCTGCGGCTACAATTCTG	83.40
CYTC_R	CCCGGAAGAGGACTTGCTT	83.40

Table 1 - Primers List

References

1. Alberti, S. G., Zimmet, P., Shaw, J. & Grundy, S. M. The IDF Consensus Worldwide Definition of the Metabolic Syndrom. 24 (2006). at <https://www.idf.org/webdata/docs/IDF_Meta_def_final.pdf>
2. Shimano, H. Pathophysiology of metabolic syndrome. *Nippon rinsho. Japanese J. Clin. Med.* **62,** 1029–1035 (2004).
3. Desvergne, B., Michalik, L. & Wahli, W. Transcriptional regulation of metabolism. *Physiol. Rev.* **86,** 465–514 (2006).
4. Rui, L. Energy Metabolism in the Liver. *NIH Public Access* **72,** 181–204 (2014).
5. Connaughton, S. *et al.* Regulation of pyruvate dehydrogenase kinase isoform 4 (PDK4) gene expression by glucocorticoids and insulin. *Mol. Cell. Endocrinol.* **315,** 159–167 (2010).
6. Jeoung, N. H. *et al.* Role of pyruvate dehydrogenase kinase isoenzyme 4 (PDHK4) in glucose homoeostasis during starvation. *Biochem. J.* **397,** 417–25 (2006).
7. Saltiel, A. R. & Kahn, C. R. Insulin signalling and the regulation of glucose and lipid metabolism. *Nature* **414,** 799–806 (2001).
8. Treyer, A. & Müsch, A. Hepatocyte polarity. *Compr. Physiol.* **3,** 243–87 (2013).
9. Yoon, J. C. *et al.* Control of hepatic gluconeogenesis through the transcriptional coactivator PGC-1. *Nature* **413,** 131–138 (2001).
10. Herzig, S. *et al.* CREB regulates hepatic gluconeogenesis through the coactivator PGC-1. *Nature* **413,** 179–83 (2001).
11. Longuet, C. *et al.* The glucagon receptor is required for the adaptive metabolic response to fasting. *Cell Metab.* **8,** 359–71 (2008).
12. Kersten, S. *et al.* Peroxisome proliferator-activated receptor alpha mediates the adaptive response to fasting. *J. Clin. Invest.* **103,** 1489–98 (1999).
13. Staels, B. & Fonseca, V. A. Bile acids and metabolic regulation: mechanisms and clinical responses to bile acid sequestration. *Diabetes Care* **32 Suppl 2,** S237-45 (2009).
14. De Fabiani, E. *et al.* When Food Meets Man: the Contribution of Epigenetics to Health. *Nutrients* **2,** 551–571 (2010).
15. Duran-Sandoval, D. *et al.* Glucose regulates the expression of the farnesoid X receptor in liver. *Diabetes* **53,** 890–8 (2004).
16. Park, W.-H. & Pak, Y. K. Insulin-dependent suppression of cholesterol 7α-hydroxlase is a possible link between glucose and cholesterol metabolisms. *Exp. Mol. Med.* **43,** 571–579 (2011).
17. Zhang, Y., Castellani, L. W., Sinal, C. J., Gonzalez, F. J. & Edwards, P. A. Peroxisome proliferator-activated receptor-gamma coactivator 1alpha (PGC-1alpha) regulates triglyceride metabolism by activation of the nuclear receptor FXR. *Genes Dev.* **18,** 157–69 (2004).
18. Kanaya, E., Shiraki, T. & Jingami, H. The nuclear bile acid receptor FXR is activated by PGC-1alpha in a ligand-dependent manner. *Biochem. J.* **382,** 913–21 (2004).
19. Godoy, P. *et al.* Recent advances in 2D and 3D in vitro systems using primary hepatocytes, alternative hepatocyte sources and non-parenchymal liver cells and their use in investigating mechanisms of hepatotoxicity, cell signaling and ADME. *Arch. Toxicol.* **87,**

1315–530 (2013).
20. Miranda, J., Cipriano, M. & Castro, M. Self-Assembled 3D Spheroids and Hollow-fibre Bioreactors improve MSC-Derived. *Arch. Toxicol.* (2016).
21. Bhatia, S. N. & Ingber, D. E. Microfluidic organs-on-chips. *Nat. Biotechnol.* **32,** 760–772 (2014).
22. Cipriano, M., Correia, J., Castro, M., Santos, J. M. & Miranda, J. P. The Role of Epigenetic Modifiers on Extended Cultures of Functional Hepatocyte-Like Cells Derived From hnMSCs. *Arch. Toxicol.* (2016).
23. Miranda, J. P. *et al.* The human umbilical cord tissue-derived MSC population UCX® promotes early motogenic effects on keratinocytes and fibroblasts and G-CSF-mediatedmobilization of BM-MSCS when transplanted in vivo. *Cell Transplant.* **24,** 865–877 (2015).
24. Santos, J. M. *et al.* 3D spheroid cell culture of umbilical cord tissue-derived MSCs (UCX®) leads to enhanced paracrine induction of wound healing. *Stem Cell Res. Ther.* **6,** 90 (2015).
25. Miranda, J. P. *et al.* Merging bioreactor technology with 3D hepatocyte-fibroblast culturing approaches: Improved in vitro models for toxicological applications. *Toxicol. Vitr.* **25,** 825–832 (2009).
26. Rajan, N., Habermehl, J., Coté, M.-F., Doillon, C. J. & Mantovani, D. Preparation of ready-to-use, storable and reconstituted type I collagen from rat tail tendon for tissue engineering applications. *Nat. Protoc.* **1,** 2753–2758 (2006).
27. Martínez-redondo, V. *et al.* Correia et al, 2015. (2015).
28. Wilkening, S., Stahl, F. & Bader, A. Comparison of primary human hepatocytes and hepatoma cell line HepG2 with regard to their biotransformation properties. *Drug Metab. Dispos.* **31,** 1035–1042 (2003).
29. Donato, M. T., Gomez-Lechon, M. J. & Castell, J. V. A microassay for measuring cytochrome P450IA1 and P450IIB1 activities in intact human and rat hepatocytes cultured on 96-well plates. (1993).
30. Miranda, J. P. *et al.* Extending Hepatocyte Functionality for Drug-Testing Applications Using High-Viscosity Alginate–Encapsulated Three-Dimensional Cultures in Bioreactors. *Tissue Eng. Part C Methods* **16,** 1223–1232 (2010).
31. Ferris, H. A. *et al*. New mechanisms of glucocorticoid-induced insulin resistance: make no bones about it. *J. Clin. Invest.* **122,** 3854–3857 (2012).
32. Estall, J. L. *et al.* PGC-1alpha negatively regulates hepatic FGF21 expression by modulating the heme/Rev-Erb(alpha) axis. *Proc Natl Acad Sci U S A* **106,** 22510–22515 (2009).
33. Monostory, K., Kőhalmy, K., Prough, R. A., Kóbori, L. & Vereczkey, L. The effect of synthetic glucocorticoid, dexamethasone on CYP1A1 inducibility in adult rat and human hepatocytes. *FEBS Lett.* **579,** 229–235 (2005).
34. Stephen C. Strom, Ljubomir A. Pisarov, Kenneth Dorko, Melissa T. Thompson, John D. Schuetz, and E. G. S. Use of Human Hepatocytes to Study P450 Gene Induction. **272,** 388–401 (1996).
35. Gomez-Lechon, M. J., Tolosa, L., Conde, I. & Donato, M. T. Competency of different cell models to predict human hepatotoxic drugs. *Expert Opin. Drug Metab. Toxicol.* **10,** 1553–1568 (2014).
36. Chivu, M. *et al.* In vitro hepatic differentiation of human bone marrow mesenchymal stem cells under differential exposure to liver-specific factors. *Transl. Res.* **154,** 122–32 (2009).
37. Polin, R., Fox, W. W. & Abman, S. H. *Fetal and Neonatal Physiology: Expert Consult - Online and Print - Richard Alan Polin, William W. Fox, Steven H. Abman - Google Livros.* (Elsevier, 2011).
38. Audet-Walsh, É. & Giguère, V. The multiple universes of estrogen-related receptor α and γ in metabolic control and related diseases. *Acta Pharmacol. Sin.* **36121,** 51–61 (2015).
39. Palou, M. *et al.* Sequential changes in the expression of genes involved in lipid metabolism in adipose tissue and liver in response to fasting. *Pflugers Arch. Eur. J. Physiol.* **456,** 825–836 (2008).
40. Iizuka, K. & Horikawa, Y. ChREBP: A Glucose-activated Transcription Factor Involved in the Development of Metabolic Syndrome. *Endocr. J.* **55,** 617–624 (2008).
41. TAL, M., KAHN, B. B. & LODISH, H. F. Expression of the Low Km GLUT-1 Glucose Transporter Is Turned on in Perivenous Hepatocytes of Insulin- Deficient Diabetic Rats*. *Endocrinology* **129,** 1933–1941 (1991).
42. Jeong, J. Y., Jeoung, N. H., Park, K.-G. & Lee, I.-K. Transcriptional regulation of pyruvate dehydrogenase kinase. *Diabetes Metab. J.* **36,** 328–35 (2012).
43. Shin, D.-J., Campos, J. A., Gil, G. & Osborne, T. F. PGC-1alpha activates CYP7A1 and bile acid biosynthesis. *J. Biol. Chem.* **278,** 50047–52 (2003).
44. Hernandez, C. *et al.* A sweet path to insulin resistance through PGC-1beta. *Cell Metab.* **9,** 215–6 (2009).
45. Meirhaeghe, A. *et al.* Characterization of the human, mouse and rat PGC1β (peroxisome- proliferator-activated receptor-γ co-activator 1β) gene in vitro and in vivo. *Biochem. J* **373,** 155–165 (2003).
46. Herzog, B. *et al.* Estrogen-related receptor alpha is a repressor of phosphoenolpyruvate carboxykinase gene transcription. *J. Biol. Chem.* **281,** 99–106 (2006).
47. Berg, J., Tymoczko, J. & Stryer, L. Biochemistry. *Biochemistry* (2002). at <http://www.ncbi.nlm.nih.gov/books/NBK21154/>
48. Girard, J. Gluconeogenesis in Late Fetal and Early Neonatal Life. *Neonatology* **50,** 237–258 (1986).
49. Foretz, M. *et al.* ADD1/SREBP-1c is required in the activation of hepatic lipogenic gene expression by glucose. *Mol. Cell. Biol.* **19,** 3760–8 (1999).
50. Azzout-Marniche, D. *et al.* Insulin effects on sterol regulatory-element-binding protein-1c (SREBP-1c) transcriptional activity in rat hepatocytes. *Biochem. J.* **350 Pt 2,** 389–93 (2000).
51. Burri, L. *et al.* The Role of PPARα Activation in Liver and Muscle. *PPAR Res.* **2010,** (2010).
52. Shipp, D. A., Parameswaran, M. & Arinze, I. J. Development of fatty acid oxidation in neonatal guinea-pig liver. *Biochem. J* **208,** 723–730 (1982).
53. Duran-Sandoval, D. *et al.* Glucose regulates the expression of the farnesoid X receptor in liver. *Diabetes* **53,** 890–8 (2004).
54. Godoy, P. *et al.* Gene network activity in cultivated primary hepatocytes is highly similar to diseased mammalian liver tissue. *Arch. Toxicol.* **90,** 2513–2529 (2016).
55. Jiang, G. & Zhang, B. B. Glucagon and regulation of glucose metabolism. *Am.J.Physiol Endocrinol.Metab* **284,** E671–E678 (2003).
56. Postic, C. *et al.* Evidence for a transient inhibitory effect of insulin on GLUT2 expression in the liver: studies in vivo and in vitro. *Biochem. J* **293,** 119–124 (1993).
57. Liu, C. & Lin, J. D. PGC-1 coactivators in the control of energy metabolism Structure and function of PGC-1. *Acta Biochim Biophys Sin* **43,** 248–257 (2011).
58. Liang, H. & Ward, W. F. PGC-1a: a key regulator of energy metabolism.
59. Zhang, M. Y. *et al.* Microfluidic environment for high density hepatocyte culture. *Biomed. Microdevices* **10,** 117–121 (2008).
60. Niiya, T. *et al*. Immediate increase of portal pressure, reflecting sinusoidal shear stress, induced liver regeneration after partial hepatectomy. *J. Hepatobiliary. Pancreat. Surg.* **6,** 275–280 (1999).
61. Zhang, C. & Noort, D. van. Cells in Microfluidics. *TripleC* **11,** 13–35 (2011).